



## CHAPTER IV

### PREPARATION OF ULTRA-FINE SILICA FIBERS USING ELECTROSPUN POLY(VINYL ALCOHOL)/SILATRANE COMPOSITE FIBERS AS PRECURSOR

#### 4.1 Abstract

Ultra-fine composite fibers made from poly(vinyl alcohol) (PVA)/silatrane, an inexpensive and moisture-stable silicon-containing compound, were prepared by a combined sol-gel processing and electrospinning technique with average diameters ranging between 119 and 405 nm. These fibers were subsequently converted to ultrafine silica fibers by calcination treatment, with the aim of producing a silica structure with a high surface area-to-mass ratio. Upon calcination at 500°C, the PVA/silica composite fibers were converted into amorphous silica fibers, while calcination of the composite fibers at temperatures  $\geq 700^\circ\text{C}$  resulted in the formation of cristobalite fibers. The average diameter of these silica fibers ranged between 162 and 213 nm.

**(Keywords:** Electrospinning; Silatrane; Silica fibers)

#### 4.2 Introduction

In the past decade, much interest has been paid to a fiber fabrication technique, commonly known as electrospinning (e-spinning), because of its ability to fabricate ultrafine fibers with diameters in the micrometer to nanometer range [1, 2]. The setup of the e-spinning process is simple, as it usually contains three major components: a high-voltage power supply, a container where a polymer liquid (i.e., a solution or melt) is placed with a small opening to be used as a nozzle, and a conductive collection device (see, e.g., Fig. 4.1). Under the influence of a high electric field, a partially spherical droplet of the polymer liquid at the capillary tip is deformed into a conical one. Further increase in the electric field causes an ejection of a charged stream of the polymer liquid (i.e., a charged jet), which deposits in a

random fashion on the collection device in the form of a nonwoven fabric [1, 2]. Because of its high surface area to volume or mass ratio, the electrospun (e-spun) fabric might be suitable for various applications, e.g., for filtration, reinforcing materials, wound dressing, tissue scaffolding, releasing carriers of drugs, and so on [3, 4].

The e-spinning process is simple enough to be further developed for the mass production of continuous, ultrafine fibers from materials of diverse origins, e.g., natural [5] or synthetic [6] polymers and sol-gel-based ceramics [7]. While the fabrication of e-spun fibers from polymeric materials is straightforward, that from the sol-gel-based ceramic counterparts can be done with two different methods, i.e., with the polymer template and the direct spinning methods. While the first method utilizes a polymeric gelator to facilitate the e-spinning of a sol solution, the second method does not. Metal oxide ceramics in the form of ultrafine fibers are finally obtained by further calcination of the obtained e-spun polymer/metal oxide gel composite fibers or the e-spun metal oxide gel fibers.

Among the various metal oxides, silica is the most commonly found compound in nature, as both sand and a major component of the cell walls of diatoms. Silica and mesoporous silica, as nanostructured entities such as nanowires and nanofibers, have attracted considerable attention because of their unique properties and wide applicability in mesoscopic research, opto- and magnetoelectronic devices, sensors, and catalysis [8, 9].

Shao et al. [8] were the first to prepare silica fibers (200–300 nm in diameters) from the e-spun silica/poly(vinyl alcohol) (PVA) composite fibers after calcination at 400°–800°C. The sol suspension was prepared from tetraethylorthosilicate (TEOS), phosphoric acid, and distilled water in the molar ratio of 1:0.01:11, and the weight ratio between silica gel and PVA in the spinning silica/PVA suspension was 59%. Choi et al. [10] prepared e-spun silica fibers (200–600 nm in diameters) directly from a sol suspension of TEOS/ethanol/distilled water/hydrochloric acid in the molar ratio of 1:2:2:0.01 without the use of any polymeric gelator. Because no polymeric gelator was used, further calcination was not necessary. Zhang et al. [11] also used the direct spinning method to prepare e-spun silica fibers from a sol suspension of TEOS/water/HCl in ethanol. The

concentrations of each component in the ethanolic solution were 1, 2, and, 0.01M, respectively.

It is evident that all of these previous reports utilized TEOS as the source of silica. As TEOS is highly sensitive to moisture, handling and controlling the property of the resulting sol suspension over the course of the fabrication process could be problematic. The use of another silica source that possesses greater stability towards moisture could alleviate such obstacles. Silatrane is one such structure that possesses a very good moisture stability property [12]. The present manuscript is, therefore, aimed at exploring the use of silatrane as the silica source for the fabrication of espun silica fibers, by using PVA as the polymeric gelator.

### 4.3 Experimental section

#### 4.3.1 Materials

Silicon dioxide (silica; amorphous precipitates; purity = 100%) was purchased from Sigma-Aldrich (Steinheim, Germany). Ethylene glycol (EG; purity = 100%) and triethanolamine (TEA; purity = 98%) were purchased from Merck (NJ). Acetonitrile (purity = 99.9%) was purchased from Labscan (Asia) (Bangkok, Thailand). PVA ( $M_w = 72,000$  Da and degree of hydrolysis  $\geq 98\%$ ) was purchased from Sigma-Aldrich. All chemicals were used as received.

#### 4.3.2 Preparation of Silatrane

The method for the preparation of silatrane was described previously [13]. Briefly, a mixture of silica (6 g, 0.10 mol) and TEA (18.6 g, 0.12 mol) was stirred vigorously in an excess amount of EG (100 cm<sup>3</sup>) and heated to 200°C for 10 h. The resulting solution was placed in vacuo to remove unreacted EG, resulting in a crude precipitate. The white solid product was washed with acetonitrile, dried in a vacuum desiccator, and characterized using a Nicolet Nexus 670 Fourier transformed infrared spectroscope (FT-IR) and a Perkin-Elmer Pyris Diamond thermogravimetric analyzer (TGA).

FT-IR: 3422 cm<sup>-1</sup> ( $\nu$ O-H), 2986–2861 cm<sup>-1</sup> ( $\nu$ C-H), 2697 cm<sup>-1</sup> ( $\nu$ N-Si), 1459–1445 cm<sup>-1</sup> ( $\nu$ C-H), 1351 cm<sup>-1</sup> ( $\nu$ C-N), 1082 cm<sup>-1</sup> ( $\nu$ Si-O-C), 579 cm<sup>-1</sup>

( $\alpha$ -N-Si) [12]. TGA: a majority of weight loss occurred at  $\sim 390$  °C with a ceramic yield of  $\sim 19\%$ – $23\%$ .

#### 4.3.3 Electrospinning of PVA/Silatrane Solutions and Preparation of Silica Fibers

The PVA/silatrane solutions were first prepared by mixing 0.5 g of silatrane with 600 ml of water. The solution was then added into 8 ml of aqueous PVA solution. The concentration of the base PVA solution was varied between 6 and 13 wt% and the resulting mixture was constantly stirred for 4 h. The as-prepared solutions are referred to as the spinning solutions.

A schematic drawing of the e-spinning setup utilized in this work is shown in Fig. 4.1. In a typical process, each of the spinning solutions was loaded into a plastic syringe. A blunt 20-G stainless-steel needle was used as a nozzle. Both the syringe and the nozzle were tilted  $\sim 45^\circ$  from a horizontal baseline to maintain the constant presence of a droplet at the tip of the nozzle. A Gamma High Voltage Research UC5-30P power supply was used to charge the spinning solution by connecting the emitting electrode of positive polarity to the nozzle and the grounding electrode to an aluminum sheet wrapped around a rigid plastic backing, used as a collection device. The distance between the tip of the nozzle and the collection device defines a collection distance.

For the preparation of the PVA/silatrane composite fibers, the following parameters were varied to investigate their effect on the morphological appearance of the obtained fibers: the concentration of the spinning solutions (i.e., 6–13 wt% of the base PVA solutions under a fixed electric field of 15 kV/10 cm), the applied electrical potential (i.e., 9–17.5 kV over a fixed collection distance of 10 cm for the spinning solution from a base PVA solution of 10 wt%), and the collection distance (i.e., 8–15 cm for the spinning solution from a base PVA solution of 10 wt% and a fixed applied potential of 15 kV). For these studies, the collection time was fixed at  $\sim 5$  min.

The PVA/silatrane composite fibers that were used to investigate the effect of calcinations temperature on the morphological appearance, properties, and structures of the postcalcined silica fibers were prepared from a spinning solution

with a concentration of base PVA solution of 10 wt% under a fixed electric field of 15 kV/10 cm. The e-spun fibers were left exposed to ambient moisture (ca. 55%  $\pm$  2% RH) for  $\sim$ 5 h and subsequently subjected to calcination in a Carbolite CFS 1200 furnace at a temperature ranging between 500° and 1100°C for 5 h to remove PVA. The heating program started from room temperature with the heating rate of 0.5°C min<sup>-1</sup>.

#### 4.3.4 Characterization

The morphological appearance and size of the e-spun PVA/ silatrane composite fibers and the as calcined silica fibers were observed by a JEOL 5200-2AE (Tokyo, Japan) scanning electron microscope (SEM). The diameters of the obtained fibers were measured directly from SEM images, using SEMAphore 4.0 software, from which the average values were calculated ( $n \geq 100$ ). The thermal behavior of the neat PVA powder and the e-spun PVA/silatrane composite fibers was investigated using TGA over a temperature range of 100°–600°C at a heating rate of 10°C/min under nitrogen atmosphere. Functional groups of the materials were observed by FT IR over the wave number range of 400–4000 cm<sup>-1</sup> at a resolution of 4 cm<sup>-1</sup> using the KBr pellet method. Specifically, each sample was thoroughly crushed, mixed with KBr at an approximate weight ratio between the sample and KBr of 1:100, and pressed into a thin pellet. Wide-angle X ray diffraction (WAXD) patterns of the ascalcined silica fibers were obtained from a Rigaku D/MAX-2000 (Tokyo, Japan) X-ray diffractometer using CuK $\alpha$  over a scanning range of 5°–70° with a scanning speed of 5° min<sup>-1</sup> and a 0.02° scanning step. WAXD was used to investigate the microstructure of the as-calcined silica fibers. Lastly, the BET surface area of both the pre- and the postcalcined fibers was measured using a Quantasorb JR Autosorp-1 gas sorption system (Quantachrome, Boynton Beach, FL). All of the samples were degassed at 300°C before measurement.

## 4.4 Results and Discussion

### 4.4.1 Electrospun PVA/Silatrane Composite Fibers

#### 4.4.1.1 *Effect of PVA Concentration*

Upon the application of a high electrical potential (i.e., 15 kV) to each of the as-prepared PVA/silatrane solutions within a finite distance between the tip of the nozzle and the collector plate (i.e., 10 cm), fibers were deposited as a nonwoven mat on the surface of the collector plate. The morphological appearance of the e-spun fiber mats from the PVA/silatrane solutions obtained from three different concentrations of base PVA solutions (i.e., 6, 10, and 13 wt%) was carefully studied (results not shown). At 6 wt% of the base PVA solution, beaded fibers were obtained. The formation of the bead-on-string morphology was postulated to result from either the viscoelastic relaxation or the work of surface tension upon partial discharge of the charged jet when it was not dry enough before deposition on the collector [14]. At 6 wt%, the diameters of the fibers were  $144 \pm 100$  nm. Despite the fact that only the fiber segments between beads were measured for diameters, the presence of the beads obviously caused the deviation of the data to be relatively large.

A further increase in the concentration of the base PVA solutions to 10 and 13 wt% resulted only in the formation of smooth fibers, with the diameters of the obtained fibers being  $142 \pm 46$  and  $405 \pm 128$  nm, respectively. Obviously, increasing the concentration of the base PVA solutions from 10 to 13 wt% caused the diameters of the e-spun fibers to increase, as expected. The observed increase in fiber diameters was a result of the increase in the viscosity of the spinning solutions, as increased viscoelastic force should prevent the jet segment from being stretched by the constant Coulombic repulsion force [6]. However, a further increase in the concentration or the viscosity of the spinning solutions could ultimately lead to nonuniform ejection of the jet when the viscosity becomes prohibitively too great.

Recently, Supaphol and Chuangchote [15] reported a careful investigation on the e-spinning of various PVA aqueous solutions, with the concentration of the solutions ranging between 6 and 14 wt%. The viscosity value of the PVA aqueous solutions increased from 62 mPa·s at a PVA concentration of 6 wt% to 2430 mPa·s at a PVA concentration of 14 wt% [15]. E-spinning of these solutions under an electric field of 15 kV/15 cm and a solution feed rate of 1 ml/h resulted in fiber mats with the average diameters of the individual fibers within the mats being 92, 285, and 527 nm at PVA concentrations of 6, 10, and 14 wt%,

respectively [15]. The slight discrepancy between the values obtained in this work and those reported in the literature [15] is likely a result of the differences in the spinning solutions and the conditions used.

#### *4.4.1.2 Effect of Applied Electrical Potential*

The effect of the electrical potential (i.e., 9 – 17.5 kV), which was applied over a collection distance of 10 cm for the spinning solution prepared from 10 wt% PVA solution, on the morphology of the e-spun fibers is shown in Fig. 4.2. Apparently, the e-spun fibers from the spinning solution fabricated under the applied electrical potential of 9 – 15 kV were smooth, while those from the solution fabricated under the applied electrical potential of 17.5 kV exhibited the bead-on-string morphology. With increasing the applied electrical potential from 9 to 15 kV, the diameters of the obtained fibers decreased from  $134 \pm 39$  to  $119 \pm 35$  nm. A further increase in the applied electrical potential to 17.5 kV resulted in an increase in the diameters of the obtained fibers to  $185 \pm 60$  nm, likely a result of the irregularity of the beaded fibers.

Increasing the applied electrical potential resulted in an increase in both the electrostatic force, which is responsible for the transport of the charged jet to the collection device, and the Coulombic repulsion force, which is responsible for the stretching of an ejected jet segment [6, 15]. The increase in both the electrostatic and the Coulombic repulsion forces could cause the diameters of the e-spun fibers to decrease (because of the increased stretching force exerted on a given jet segment) [6, 15]. On the other hand, the increase in the electrostatic force could also cause the diameters of the e-spun fibers to increase, a phenomenon that results from the increase in both the speed of the jet segment and the mass flow rate, which in turn causes the onset of the bending instability to occur closer to the collection device [6, 15]. Based on such a postulation, the observed decrease in fiber diameters with the initial increase of applied electrical potential could be attributed to the increase in both the electrostatic and the Coulombic repulsion forces, while the observed increase in fiber diameters resulting from the further increase of applied electrical potential could be attributed to the increase in the electrostatic force [15].

#### *4.4.1.3 Effect of Collection Distance*

The effect of collection distance (i.e., 8–15 cm) for the spinning solution prepared from 10 wt% PVA solution under the applied electrical potential of 15 kV on the morphology of the e-spun fibers was also investigated (results not shown). Obviously, all of the obtained fibers were smooth. The diameters of these fibers were  $229 \pm 85$ ,  $119 \pm 35$ , and  $167 \pm 73$  nm for the fibers that were e-spun at collection distances of 8, 10, and 15 cm, respectively. Although no particular relationship between the average diameter of the PVA/silatrane composite fibers and the collection distance was observed, Supaphol and Chuangchote [15] clearly showed that the average diameter of the e-spun fibers from sonicated 10 wt% PVA solution under the electrical potential of 15 kV monotonously decreased with an increase in the collection distance (i.e., from 188 nm at 7.5 cm to 163 nm at 15 cm, in particular).

#### 4.4.2 Preparation of Silica Fibers

##### 4.4.2.1 *Effect of Calcination Temperature*

The PVA/silatrane composite fibers used to investigate the effect of calcination temperature on the morphological appearance, properties, and structures of the postcalcined fibers were fabricated from the spinning solution with the concentration of base PVA solution of 10 wt% under the applied electric field of 15 kV/10 cm. Figure 4.3 shows selected SEM images of the e-spun PVA/silatrane composite fibers and the fibers that had been calcined at different temperatures in the range of 500°–1100°C. The obtained PVA/silatrane composite fibers (see Fig. 4.3(a)) were smooth, with diameters of  $210 \pm 71$  nm. Upon calcination, the fibrous nature of the original composite fibers was retained, but the as-calcined fibers shrank considerably (see Figs. 4.3(b)–(f)) because of the decomposition of the organic PVA content within. Emphatically, increasing the calcination temperature from 500° to 1100°C caused the diameters of the as calcined fibers to decrease monotonously from  $213 \pm 53$  to  $162 \pm 40$  nm.

Figure 4.4 shows TGA thermograms of pure PVA powder and the e-spun PVA/silatrane composite fibers. Evidently, the pure PVA powder exhibited two steps in the loss of its weight at temperatures ca. 255° and 435°C,



corresponding to the thermal decomposition of side groups and the main chain, respectively [16]. Shao et al. [17] reported that e-spun PVA ( $M_n = 86,000$  Da) fibers also showed two steps in the loss of their weight at temperatures ca.  $350^\circ$  and  $450^\circ\text{C}$ . The discrepancy between the values observed in this work and those reported in the literature [17] could be due to the difference in the molecular weights of the polymer used. On the other hand, for the e-spun PVA/silatrane composite fibers, three steps in the loss of their weight were observed.

While both the second and the third steps should correspond to the thermal decomposition of the native PVA, the first step between  $\sim 140^\circ$  and  $\sim 220^\circ\text{C}$  should correspond to the loss of the organic contents associated with the hydrolysis of silatrane and/or to the evaporation of trapped solvent. A similar result was also reported by Shao et al. [17], even though a different compound, i.e., TEOS, was used as the silica source. As shown by the results in Fig. 4.4, the thermal decomposition of PVA was considered complete at  $\sim 475^\circ\text{C}$ , so the as-calcined fibers should be free from the organic matter of PVA.

The chemical integrity of both the pre- and the postcalcined fibers was further investigated by FT-IR, shown in Fig. 4.5. Apparently, the postcalcined fibers exhibited an absorption peak at ca.  $1100\text{ cm}^{-1}$ , which is much more pronounced than that observed in the spectrum of the precalcined, composite fibers. Shao et al. [17] also found that the relative intensity of the peak at  $1100\text{ cm}^{-1}$  became more evident with an increase in the silica content within the e-spun PVA/silica composite fibers, which they attributed to the formation of either Si–O–C or Si–O–Si bonds. In addition to this absorption peak, the peaks at ca.  $485$  and  $795\text{ cm}^{-1}$ , which were absent in the spectrum of the precalcined, composite fibers, were clearly visible in the spectra of the as calcined fibers. Emphatically, these three absorption peaks that are associated with the Si–O–Si bonds [16] became more evident in the spectra of the fibers that had been calcined at temperatures  $\geq 700^\circ\text{C}$ . Interestingly and surprisingly, an additional absorption peak at ca.  $623\text{ cm}^{-1}$ , corresponding to the pseudolattice vibration of  $\beta$ -cristobalite [18], a high-temperature polymorph of quartz and tridymite, was observed in the spectra of the fibers that had been calcined at temperatures  $> 500^\circ\text{C}$ .

Shao et al. [8] reported that the PVA/silica composite fibers that had been calcined at temperatures of 550° and 800°C showed no evidence of the absorption peaks associated with the polymeric gelator, as only the peaks at ca. 460, 770, and 1100  $\text{cm}^{-1}$ , corresponding to the Si–O–Si bonds, were observed. In separate papers, Choi et al. [10] and Zhang et al. [11] reported that the e-spun silica fibers that had been prepared from the direct spinning method (without the use of a polymeric gelator) also exhibited three strong absorption peaks, at 790, 935, and 1043  $\text{cm}^{-1}$  and 795, 950, and 1058  $\text{cm}^{-1}$ , respectively, which corresponded to the bending and vibrational modes of the Si–O–Si bonds. These results confirmed a complete hydrolysis of TEOS without the need of further calcination of the e-spun fibers. Based on the TGA and the FT-IR results obtained in this work and the reported findings in the literature [8, 10, 11], it can be concluded at this point that the postcalcined fibers were free from organic residues and the as-calcined fibers were present in either the amorphous silica and/or the  $\beta$ -cristobalite form.

The structural organization of the postcalcined fibers was further investigated with WAXD, and the results are shown in Fig. 4.6. Only one broad scattering peak, centering at  $\sim 20^\circ$ , was observed for the fibers that had been calcined at 500°C, which could be an indication of the amorphous nature of the obtained silica fibers at such a temperature. Interestingly, at calcinations temperatures  $> 500^\circ\text{C}$ , four major diffraction peaks, characteristic of a crystalline nature of some sorts, were observed at the  $2\theta$  angles of 21.9°, 28.3°, 31.2°, and 36.0°. While the peaks at 21.9° and 36.0° could be both assigned to the (101) and (200) planes of  $\alpha$ -cristobalite and the (111) and (220) planes of  $\beta$ -cristobalite [19–20], the peaks at 28.3° and 31.2° could be assigned to reflection planes of  $\alpha$ -cristobalite [19]. The WAXD results showed that the silica fibers that had been calcined over the temperature range of 700 °–1100 °C were present in both  $\alpha$ - and  $\beta$ -cristobalite crystal forms. Moreover, for the fibers that had been calcined at 700 ° and 800 °C, another low-intensity peak at 25.9°, which could be assigned to a reflection of quartz, was observed. Clearly, the intensity of the peak was more pronounced at 700°C.

$\beta$ -Cristobalite was found to exist after amorphous silica powder had been calcined at temperatures  $\geq 1100^\circ\text{C}$ , with evidence of its a

polymorph being observed when the amorphous silica powder was calcined at temperatures  $\geq 1350^\circ\text{C}$  [19]. Under hydrothermal conditions, however,  $\beta$ -Cristobalite was observed when silica gel was treated hydrothermally with either potassium fluoride or sodium fluoride at  $300^\circ\text{C}$  for 24 h [20]. Increasing the treatment temperature to  $400^\circ\text{C}$  or changing the treating solution to sodium hydroxide resulted in the formation of quartz, which is the more thermodynamically stable crystalline form [20]. In fact, when amorphous silica was crystallized in an alkaline condition, the path of crystallization was always amorphous silica-cristobalite-quartz [21]. Based on the evidence reported in the literature [19–21] and the WAXD results obtained in this work, it is postulated that the use of silatrane as the source of silica favors the formation of cristobalite. Notwithstanding, the observation of a quartz reflection peak for the fibers that had been calcined at  $700^\circ\text{C}$  suggests that, at certain conditions such as this, quartz could be formed along with cristobalite, although in a much lesser extent.

Lastly, the BET surface area of both the pre- and the postcalcined fibers was investigated. Such a value for the e-spun PVA/silatrane composite fibers was ca.  $11\text{ m}^2/\text{g}$ , while such values for the silica fibers that had been calcined at  $500^\circ$ ,  $700^\circ$ , and  $1100^\circ\text{C}$  were 285, 198, and  $87\text{ m}^2/\text{g}$ , respectively. The observed decrease in the BET surface area with increasing calcinations temperature is likely a result of the increase in the grain size of cristobalite crystals.

#### 4.5 Conclusions

Ultrafine silica fibers were successfully prepared by the calcinations of e-spun PVA/silatrane composite fibers at various temperatures ranging between  $500^\circ$  and  $1100^\circ\text{C}$ . The diameters of the composite fibers increased with an increase in the concentration of the base PVA solution, while they decreased with an increase in the applied electrical potential. Regardless of the spinning conditions investigated, the average diameters of the composite fibers ranged between 119 and 405 nm. Upon calcination, the obtained fibers shrunk considerably because of the loss of the organic content. The average diameter of the postcalcined fibers (based on the composite

fibers that had been prepared from the e-spinning of PVA (10 wt%)/silatrane solution under the applied electric field of 15 kV/10 cm) decreased from 213 at a calcination temperature of 500°C to 162 nm at 1100°C. Both FT-IR and WAXD results confirmed that the microstructure of the fibers, obtained from the composite fibers and calcined at temperatures  $\geq 700^\circ\text{C}$ , were composed predominately of cristobalite, a high-temperature polymorph of crystalline silica. Lastly, the BET surface areas of the silica fibers ranged between 87 and 285 m<sup>2</sup>/g.

#### 4.6 Acknowledgements

This research work was supported by (1) The National Center for Petroleum, Petrochemicals and Advanced Materials (C-PPAM), Chulalongkorn University, (2) The Ratchadapisake Sompote Fund, Chulalongkorn University, and (3) The Thailand Research Fund (TRF).

#### 4.7 References

1. J. Doshi and D. H. Reneker, "Electrospinning Process and Applications of Electrospun Fibers", *J. Electrostat.*, **35**, 151–160 (1995).
2. D. H. Reneker and I. Chun, "Nanometer Diameter Fibers of Polymer, Produced by Electrospinning", *Nanotechnology*, **7**, 216–223 (1996).
3. Z. M. Huang, Y. Z. Zhang, M. Kotaki, and S. Ramakrishna, "A Review on Polymer Nanofibers by Electrospinning and Their Applications in Nanocomposites", *Compos. Sci. Technol.*, **63**, 2223–2253 (2003).
4. K. Jayaraman, M. Kotaki, Y. Zhang, X. Mo, and S. Ramakrishna, "Recent Advances in Polymer Nanofibers", *J. Nanosci. Nanotechnol.*, **4**, 52–65 (2004).
5. P. Sangsanoh and P. Supaphol, "Stability Improvement of Electrospun Chitosan Nanofibrous Membranes in Neutral or Weak Basic Aqueous Solutions", *Nanotechnology*, **7**, 2710–2714 (2006).

6. C. Mit-upatham, M. Nithitanakul, and P. Supaphol, "Ultrafine Electrospun Polyamide-6 Fibers: Effect of Solution Conditions on Morphology and Average Fiber Diameter", *Macromol. Chem. Phys.*, **205**, 2327–2338 (2004).
7. J. Watthanaarun, V. Pavarajarn, and P. Supaphol, "Titanium (IV) Oxide Nanofibers by Combined Sol–Gel and Electrospinning Techniques: Preliminary Report on Effects of Preparation Conditions and Secondary Metal Dopant", *Sci. Technol. Adv. Mater.*, **6**, 240–245 (2005).
8. C. Shao, H.-Y. Kim, J. Gong, and D.-R. Lee, "A Novel Method for Making Silica Nanofibres by using Electrospun Fibres of Polyvinylalcohol/Silica Composite as Precursor", *Nanotechnology*, **13**, 635–637 (2002).
9. Y. Zhao, H. Wang, X. Lu, X. Li, Y. Yang, and C. Wang, "Fabrication of Refining Mesoporous Silica Nanofibers via Electrospinning", *Mater. Lett.*, **62**, 143–146 (2008).
10. S. S. Choi, S. G. Lee, S. S. Im, S. H. Kim, and Y. L. Joo, "Silica Nanofibers from Electrospinning/Sol–Gel Process", *J. Mater. Sci. Lett.*, **22**, 891–893 (2003).
11. G. Zhang, W. Kataphinan, R. Teye-Mensah, P. Katta, L. Khatri, E. A. Evans, G. G. Chase, R. D. Ramsier, and D. H. Reneker, "Electrospun Nanofibers for Potential Space-Based Applications", *Mater. Sci. Eng. B*, **116**, 353–358 (2005).
12. P. Phitiyawirut, A. M. Jamieson, and S. Wongkasemjit, "VS-1 Zeolite Synthesized Directly from Silatrane", *Micropor. Mesopor. Mater.*, **77**, 203–213 (2005).
13. P. Piboonchaisit, S. Wongkasemjit, and R. Laine, "A Novel Route to Tris (Silatranxyloxy-I Propyl)Amine Directly from Silica and Triisopropanolamine, Part I", *Science Asia (formerly, J. Sci. Soc. Thailand)*, **25**, 113–119 (1999).
14. H. Fong, I. Chun, and D. H. Reneker, "Beaded Nanofibers Formed during Electrospinning", *Polymer*, **40**, 4585–4592 (1999).
15. P. Supaphol and S. Chuangchote, "On the Electrospinning of Poly (Vinyl Alcohol) Nanofibers Mats: A Revisit", *J. Appl. Polym. Sci.*, **108**, 969–978 (2008).

16. K. Nakane, T. Yamashita, K. Iwakura, and F. Suzuki, "Properties and Structure of Poly(Vinyl Alcohol)/Silica Composites", *J. Appl. Polym. Sci.*, **74**, 133–8 (1999).
17. C. Shao, H.-Y. Kim, J. Gong, B. Ding, D.-R. Lee, and S.-J. Park, "Fiber Mats of Poly(Vinyl Alcohol)/Silica Composite via Electrospinning", *Mater. Lett.*, **57**, 1579–1584 (2003).
18. M. Sitarz, M. Handke, and W. Mozgawa, "Identification of Silicoxygen in SiO<sub>2</sub> Based on IR Spectra", *Spectrochim. Acta*, **56A**, 1819–1823 (2000).
19. W. M. Kriven and S.-J. Lee, "Toughening of Mullite/Cordierite Laminated Composites by Transformation Weakening of b-Cristobalite Interphases", *J. Am. Ceram. Soc.*, **88**, 1521–1528 (2005).
20. Y. Zhu, K. Yanagisawa, A. Onda, and K. Kajiyoshi, "The Preparation of Nano-Crystallized Cristobalite Under Hydrothermal Conditions", *J. Mater. Sci.*, **40**, 3829–3831 (2005).
21. S. Campbell and W. S. Fyfe, "Hydroxyl Ion Catalysis of the Hydrothermal Crystallization of Amorphous Silica: A Possible High Temperature pH Indicator", *Am. Mineral.*, **45**, 464–468 (1960).

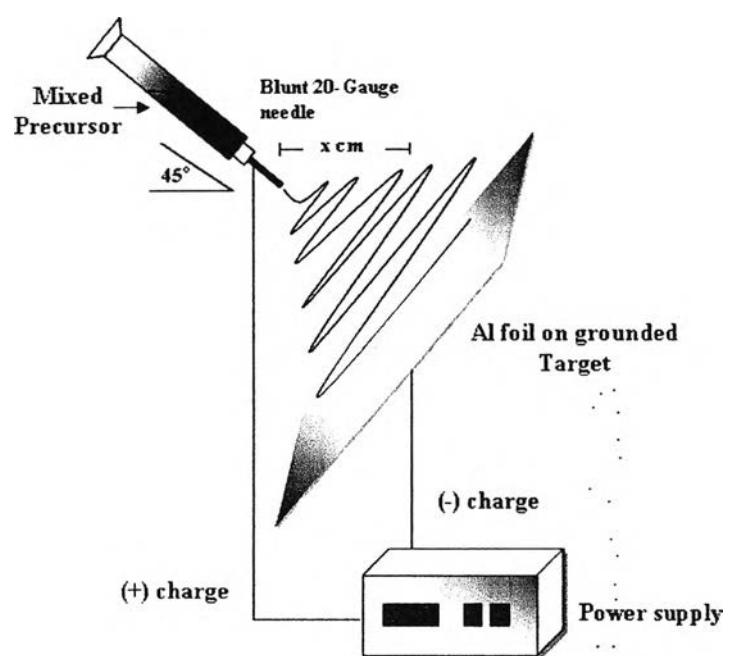


**Figure 4.1** Schematic drawing of the electrospinning apparatus utilized in this work

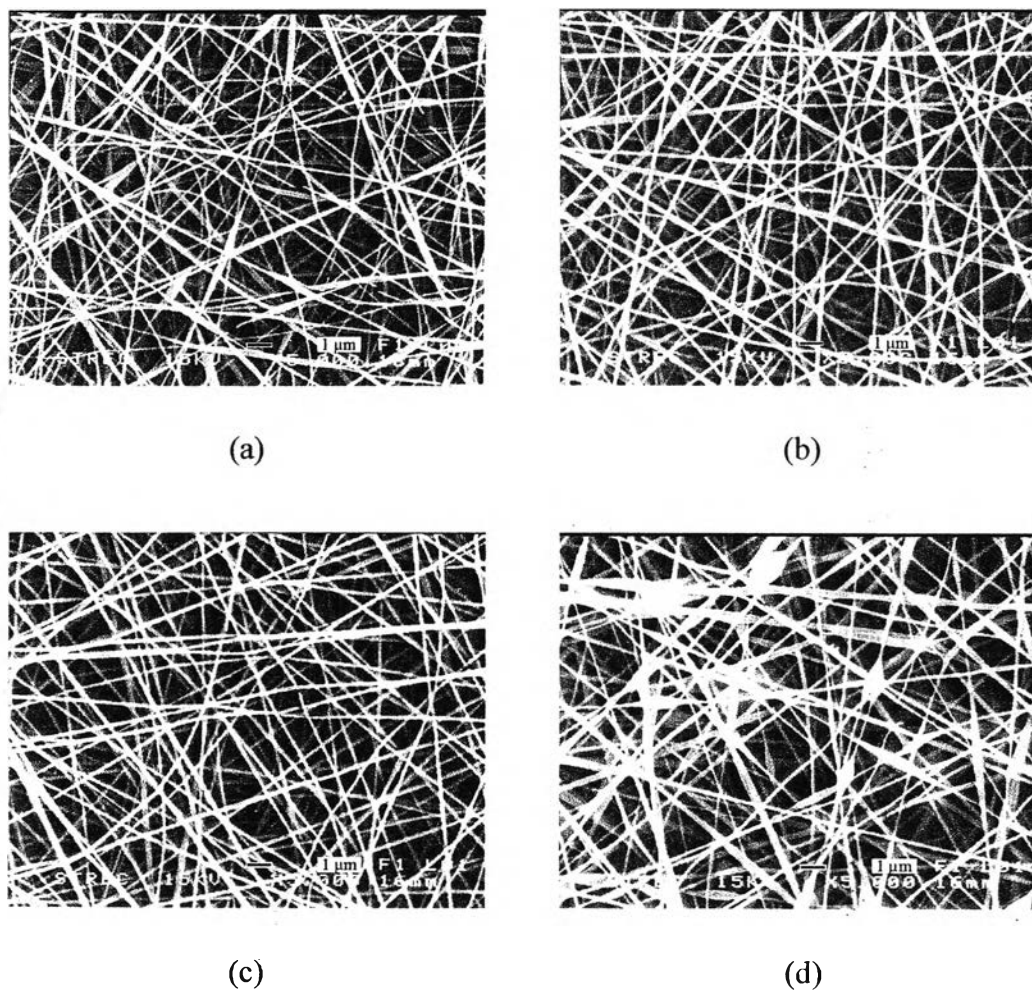


**Figure 4.2** Selected SEM images illustrating the morphological appearance of electrospun fibers from PVA (10 wt%)/silatrane solution under various electrical potentials of (a) 9, (b) 12.5, (c) 15, and (d) 17.5 kV that were applied over a fixed collection distance of 10 cm. The diameters of these fibers were  $134 \pm 39$ ,  $128 \pm 51$ ,  $119 \pm 35$ , and  $185 \pm 60$  nm, respectively.



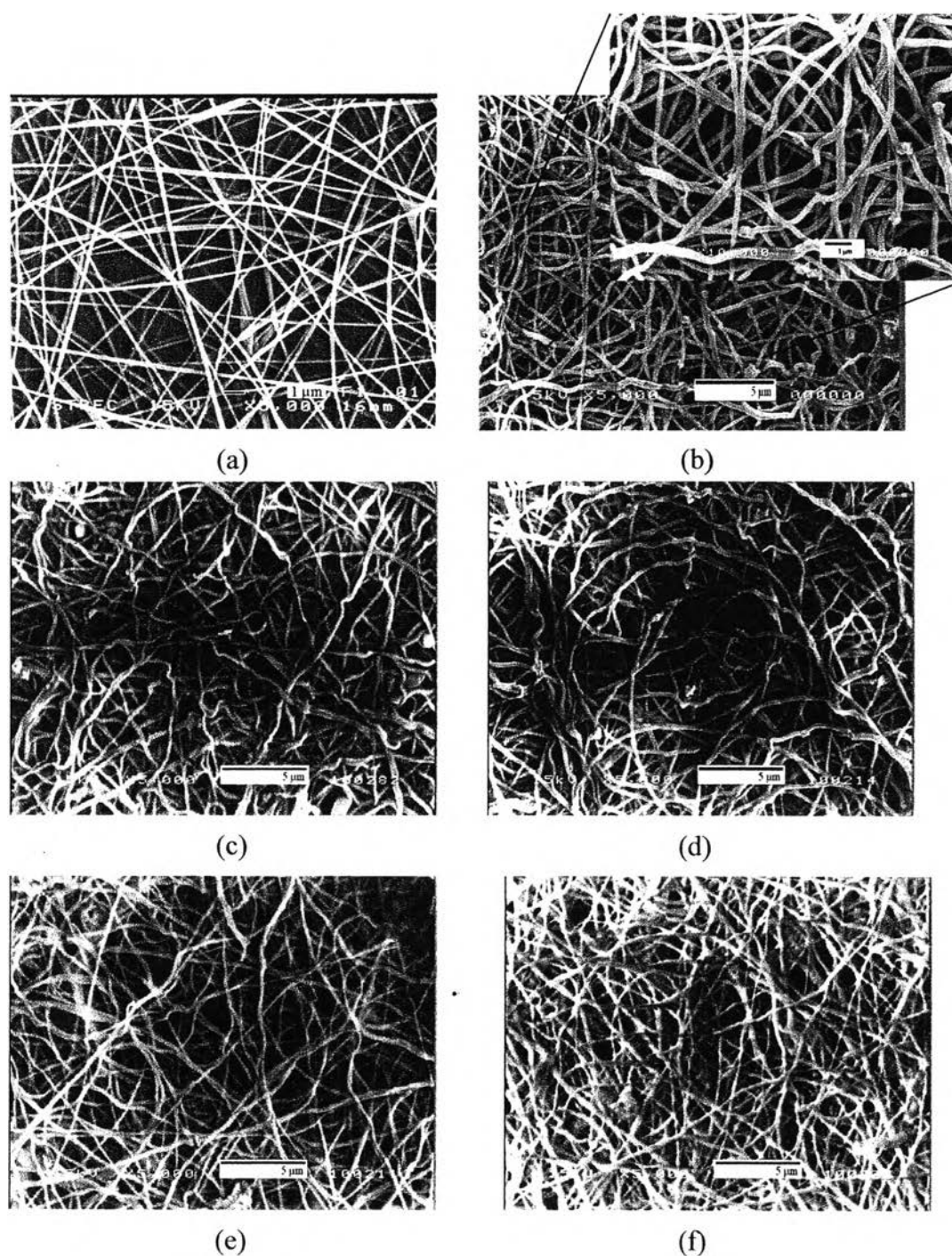


**Figure 4.3** Selected SEM images illustrating the morphological appearance of (a) pre-calcined electrospun PVA/silatrane composite fibers prepared from PVA (10 wt%)/silatrane solution under the applied electric field of 15 kV/10 cm and silica fibers that were obtained from calcination of (a) at various temperatures of (b) 500, (c) 700, (d) 800, (e) 1000, and (f) 1100°C. The diameters of these fibers were  $210 \pm 71$ ,  $213 \pm 53$ ,  $201 \pm 63$ ,  $195 \pm 48$ ,  $182 \pm 47$ , and  $162 \pm 40$  nm, respectively.

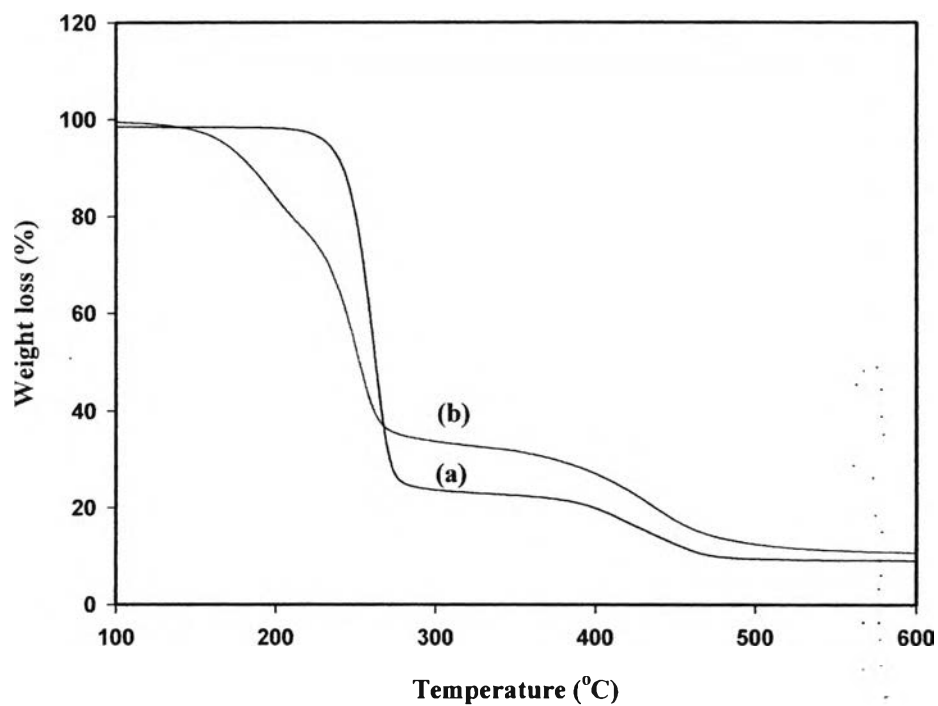


**Figure 4.4** Thermogravimetric analysis of (a) pure PVA powder and (b) pre-calcined electrospun PVA/silatrane composite fibers prepared from PVA (10 wt%)/silatrane solution under the applied electric field of 15 kV/10 cm.

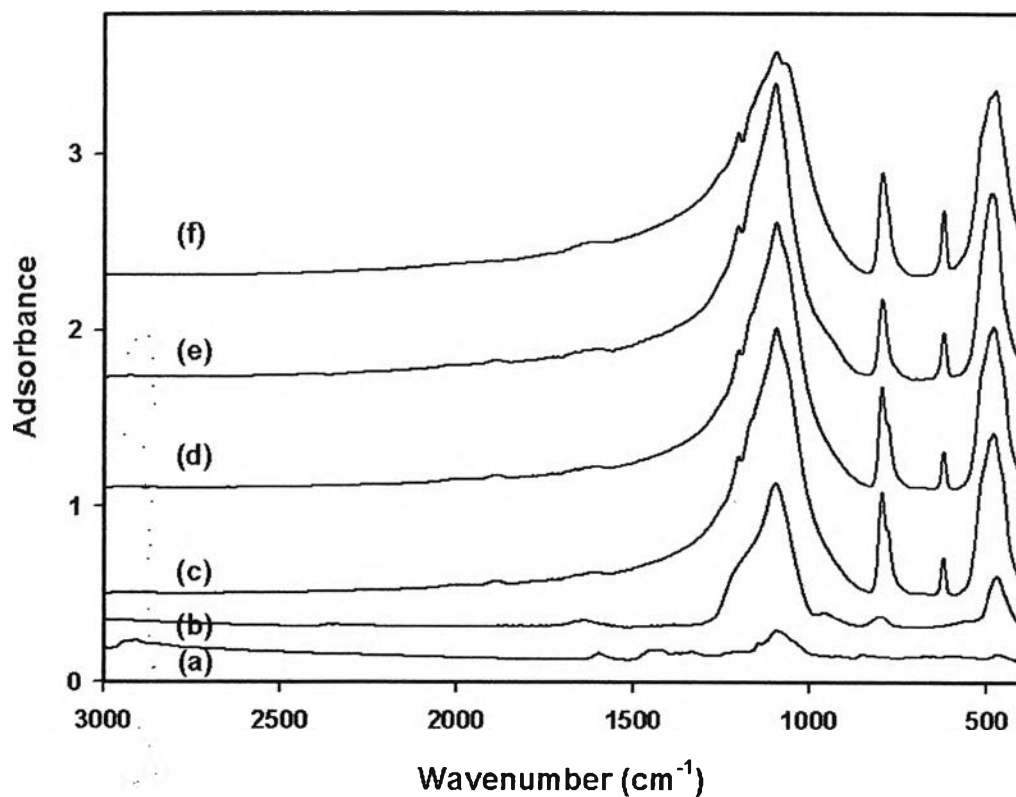


**Figure 4.5** FT-IR spectra of (a) pre-calcined electrospun PVA/silatrane composite fibers prepared from PVA (10 wt%)/silatrane solution under the applied electric field of 15 kV/10 cm and silica fibers obtained from calcination of (a) at various temperatures of (b) 500°, (c) 700°, (d) 800°, (e) 1000°, and (f) 1100°C.

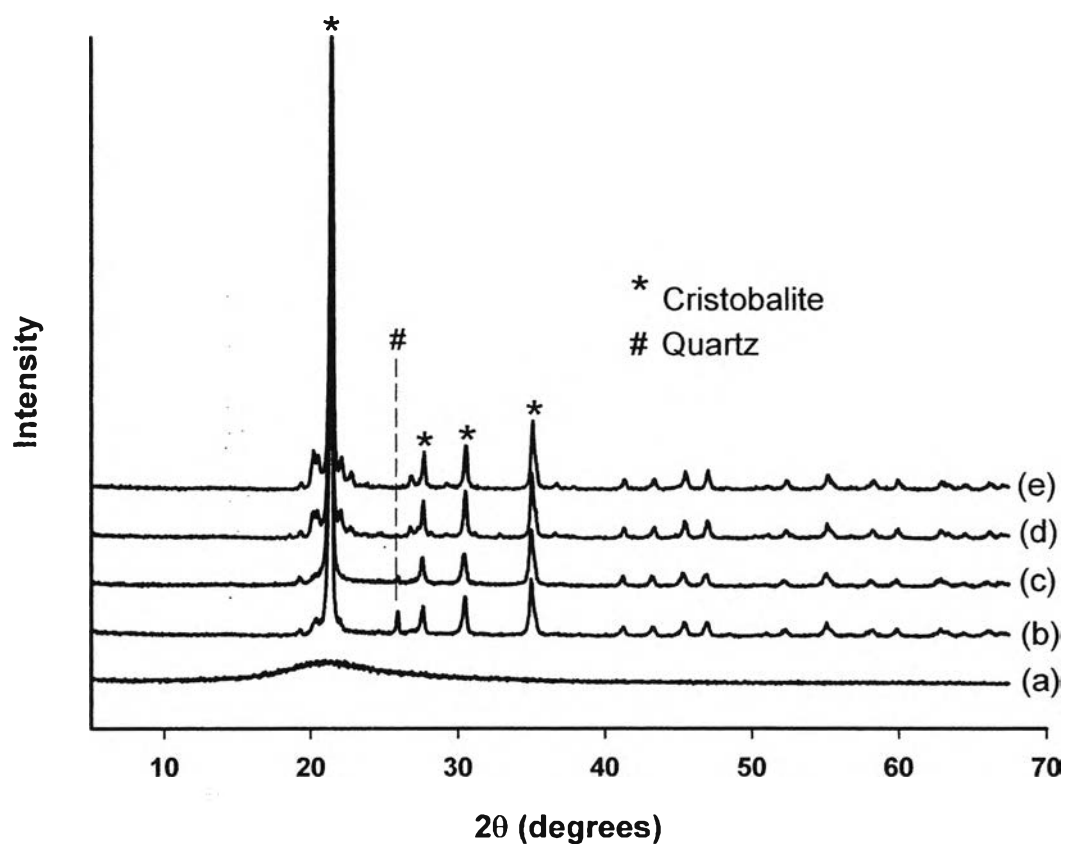


**Figure 4.6** WAXD patterns of silica fibers obtained from calcination of electrospun PVA/silatrane composite fibers prepared from PVA (10 wt%)/silatrane solution under the applied electric field of 15 kV/10 cm at various temperatures of (a) 500°, (b) 700°, (c) 800°, (d) 1000°, and (e) 1100°C.